

Chapter 3

Dry and Moist Atmospheric Convection

3.1 Convection in an incompressible fluid

In an incompressible fluid the density of fluid parcels doesn't change. However, different parts of the fluid may have different densities. Imagine, for instance, ocean water, with variable distributions of temperature and salinity (salt content). Both of these factors affect the density of ocean water. However, to a good approximation, this density is maintained as parcels move up and down to different pressure levels.

Figure 3.1 shows what happens to a fluid parcel displaced vertically for two different cases of density stratification in an incompressible fluid in a gravitational field. In the left panel the density of the displaced parcel, which doesn't change as a result of the displacement, is greater than that of the surrounding environment if the displacement is upward. As a result, the buoyancy force is downward, accelerating the parcel back toward its initial level. A downward displacement results in an upward force, which also tends to return the parcel to its initial level. The fluid in this case is *statically stable*. The opposite holds in the right panel, where a vertical displacement, either upward or downward, results in a buoyancy force which tends to reinforce the initial displacement. This is the *statically unstable* case. It is clear from figure 3.1 that static stability occurs when the density decreases with height, whereas static instability is associated with density increasing with height.

In the stable case the fluid parcel oscillates up and down about the equilibrium point. If the density profile has the form $\rho = \rho_0 + \Gamma z$, where ρ_0 is the ambient fluid density at height $z = 0$, then displacing a parcel from this level results in a buoyancy force per unit mass of $F = g(\rho_0 - \rho)/\rho = -g\Gamma z/\rho$. If no other forces are acting on the parcel, then the parcel displacement is governed by

$$\frac{d^2 z}{dt^2} = -\frac{g\Gamma}{\rho} z. \quad (3.1)$$

If the density changes only weakly with height, then we can consider ρ in the denominator of the above equation to be essentially constant, and we have a harmonic oscillator equation with oscillation frequency

$$N = \left(\frac{g\Gamma}{\rho} \right)^{1/2}. \quad (3.2)$$

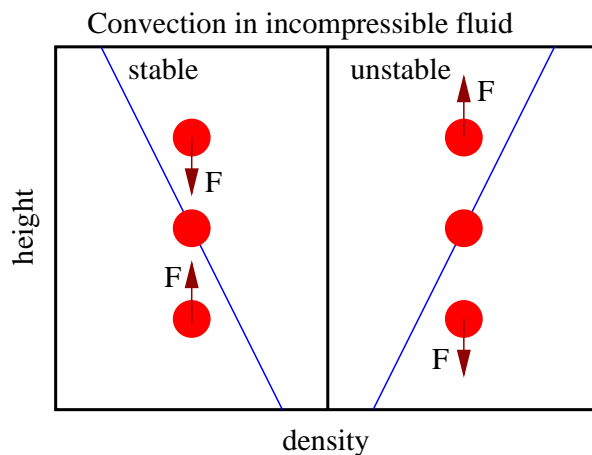


Figure 3.1: Stability and instability of a vertically displaced parcel in a stratified, incompressible fluid.

This is called the *Brunt-Väisälä* or *buoyancy* frequency, and it is the oscillation frequency of a parcel displaced vertically in an incompressible fluid and released.

The case of unstable stratification is represented by negative values of Γ . In this case equation (3.1) has solutions of the form

$$z = a \exp(\sigma t) + b \exp(-\sigma t) \quad (3.3)$$

where $\sigma = (-g\Gamma/\rho)^{1/2}$ and a and b are constants. The exponential growth in vertical displacement represents the onset of convective overturning. This solution is only valid for very small displacements. When displacements become large, nonlinear effects become important and the behavior of the fluid becomes much more complex.

3.2 Dry atmospheric convection

Air is compressible, which makes atmospheric convection somewhat more complex than that which occurs in an incompressible fluid such as water.¹ In particular, the density of an air parcel is not conserved in vertical displacements. Thus, in computing the buoyancy of a displaced air parcel, the change in buoyancy of the air parcel with height must be considered along with the vertical profile of the density of ambient air.

If no condensation occurs, then the dry entropy is conserved by vertically displaced parcels, and one must simply convert a difference in entropy between the parcel and its environment to a difference in density. Eliminating T in favor of ρ in the dry entropy equation results in

$$s_d = C_{vd} \ln(p/p_R) - C_{pd} \ln(\rho/\rho_R). \quad (3.4)$$

¹Even water is slightly compressible. However, this is only of practical importance in geophysical fluid dynamics for processes which involve large vertical displacements in deep oceans.

A small difference between the parcel and the environment at a fixed pressure is obtained by taking the differential of this equation with $\delta p = 0$:

$$\delta s_d = -\frac{C_{pd}\delta\rho}{\rho}. \quad (3.5)$$

However, this difference can be related to the vertical parcel displacement z by

$$\delta s_d = -\frac{ds_d}{dz}z. \quad (3.6)$$

Combining these equations one may compute the buoyancy force per unit mass as previously, resulting in

$$F = -\frac{g\delta\rho}{\rho} = \frac{g}{C_{pd}}\delta s_d = -\frac{g}{C_{pd}}\frac{ds_d}{dz}z \quad (3.7)$$

and a value for the buoyancy frequency of

$$N = \left(\frac{g}{C_{pd}} \frac{ds_d}{dz} \right)^{1/2}. \quad (3.8)$$

3.3 Saturated environment

Imagine now a completely saturated environment. In this environment the total entropy s is conserved by parcels, and furthermore $s = s_s$. Proceeding as before and using the approximate formula for saturated entropy, the difference between parcel and environmental values of saturated entropy at constant pressure is

$$\delta s_s \approx \left(\frac{C_{pd}}{T} + \frac{L}{T_R} \frac{dr_s}{dT} \right) \delta T. \quad (3.9)$$

Using $r_s = \epsilon e_s(T)/p$ and $d \ln(e_s)/dT = L/(R_v T^2)$, this becomes

$$\delta s_s \approx \left(C_{pd} + \frac{L_R^2 r_s}{R_v T_R^2} \right) \frac{\delta T}{T_R} \approx - \left(C_{pd} + \frac{L_R^2 r_s}{R_v T_R^2} \right) \frac{\delta\rho}{\rho}, \quad (3.10)$$

where consistent with earlier approximations, T has been set to T_R and where we approximate L by its value at T_R : $L \approx L(T_R) \equiv L_R$. It should be recalled that this is an approximate result based on a simplified formula for the total entropy.

The buoyancy force per unit mass on a parcel with a saturated entropy differing from that of the environment by δs_s is therefore

$$F = -\frac{g\delta\rho}{\rho} \approx g \left(C_{pd} + \frac{L_R^2 r_s}{R_v T_R^2} \right)^{-1} \delta s_s \quad (3.11)$$

and the buoyancy frequency in the statically stable case is

$$N \approx \left[g \left(C_{pd} + \frac{L_R^2 r_s}{R_v T_R^2} \right)^{-1} \frac{ds_s}{dz} \right]^{1/2}. \quad (3.12)$$

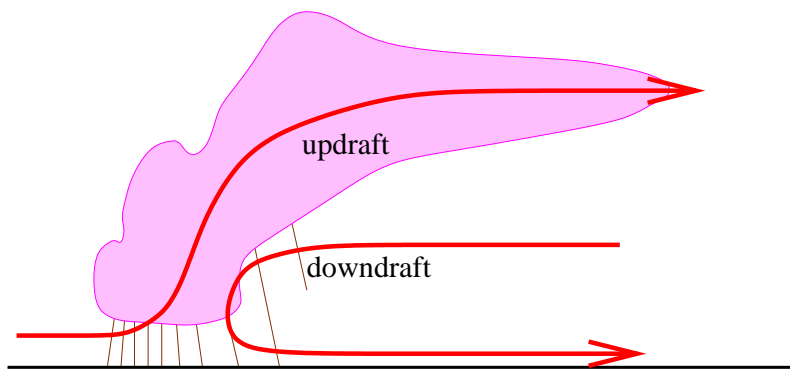


Figure 3.2: Schematic illustration of circulations in precipitating moist convection.

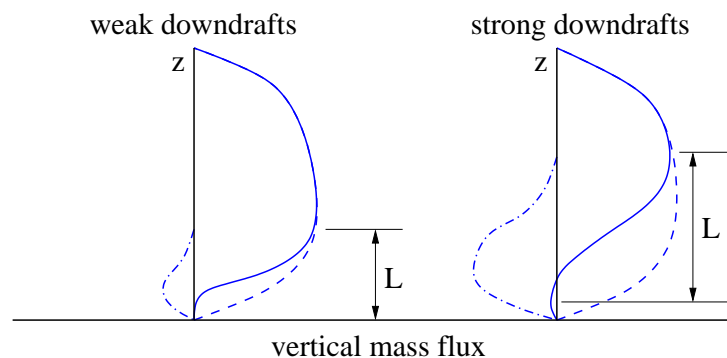


Figure 3.3: Net vertical mass flux in precipitating convection with typical updrafts (dashed lines) and weak or strong downdrafts (dot-dashed lines). The depth of the inflow layer is L .

3.4 Effects of convective rainfall

Figure 3.2 shows the dominant circulations which occur in precipitating convective systems. The updraft branch begins at low levels and ends at high levels. The moist downdraft branch is caused to descend by the cooling effects of evaporating rainfall. It enters the system at middle levels and exits at low levels.

The profile of vertical mass flux in precipitating convection is illustrated schematically in figure 3.3. If downdrafts are weak, the inflow layer is shallow, as moist inflowing air is entering updrafts, and convective instability generally only exists for parcels near the surface. Downdrafts tend to tap low-entropy air from middle levels, which mean that convection with strong downdrafts exhibit inflow through a deep layer.

Precipitating convection is unlike dry or moist non-precipitating convection, in that the balance of the compensating downward motion not taken up by the convective downdraft occurs in the dry, statically stable surroundings. As we shall see later, this stable descent is therefore spread over a very large horizontal scale, perhaps thousands of kilometers in the tropics. The entire convective circulation thus has both small-scale and large-scale aspects, making it a very difficult computational problem.

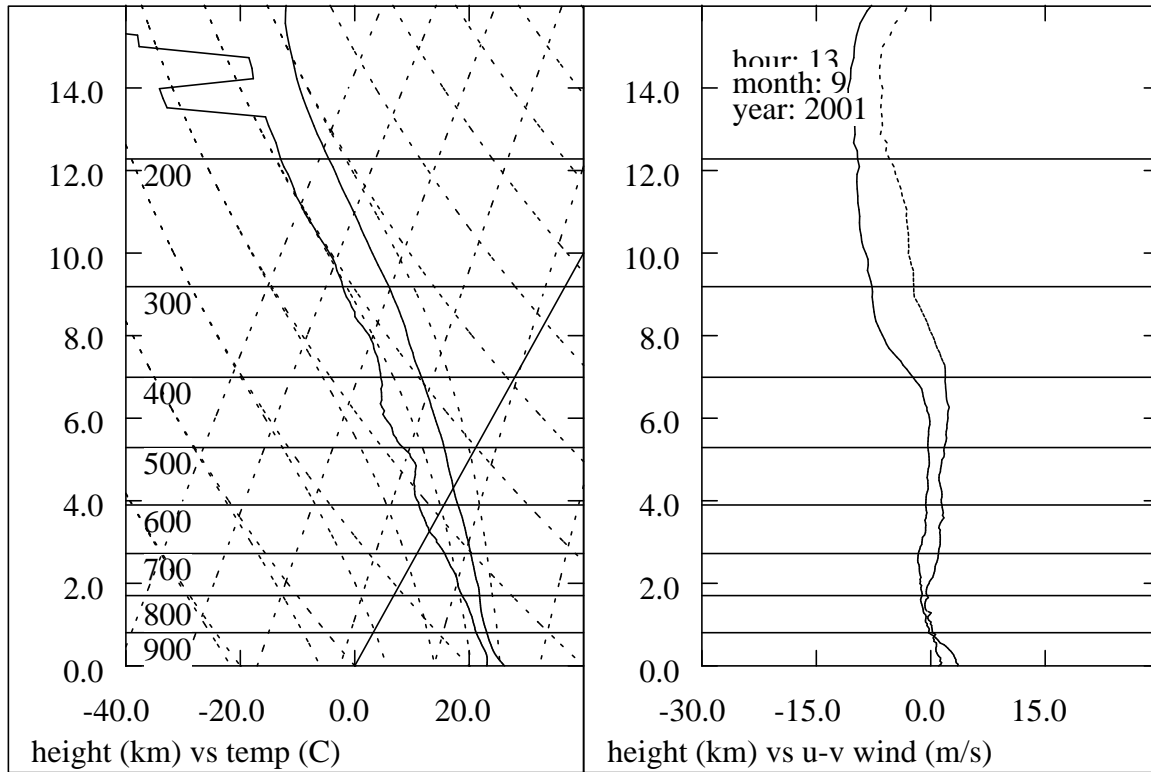


Figure 3.4: Skew T-log p chart showing mean wind and thermodynamic soundings from the summertime eastern tropical Pacific.

3.5 Thermodynamic charts

Thermodynamic charts allow parcel transformations to be obtained graphically. There are many such charts, each with advantages and disadvantages. We will consider a few. Hess (1959) presents a more extensive discussion of such charts.

3.5.1 Skew T-log p chart

The skew T-log p chart is commonly used in the United States. The behavior of parcels is followed on a chart in which temperature is plotted on the horizontal axis versus the log of pressure on the vertical axis. The lines of constant temperature are tilted to the right for convenience (“skew T”), but this not essential in understanding the properties of this chart.

To understand the basic motivation for this chart, we note that the buoyancy work done per unit mass on an ascending parcel is

$$dw = \frac{g\Delta T}{T}dz = -\frac{g\Delta T}{T}\frac{dp}{g\rho} = -\frac{R_d\Delta T}{p}dp = -R_d\Delta T d\ln p \quad (3.13)$$

where ΔT is the temperature difference between the parcel and its surroundings. The hydrostatic law has been used in deriving this as well as the ideal gas law for dry air. The effect of water vapor on density has been ignored. However, this last assumption may be removed

by substituting virtual temperature for temperature. Thus, the work done by buoyancy on a parcel in ascent is equal to the area between the environmental profile and the trajectory in $T - \ln p$ space of the ascending parcel.

The total buoyancy work done on a parcel ascending from pressure level p_1 to pressure level p_2 where buoyancy equilibrium (i. e., $\Delta T = 0$) at both levels is

$$w = - \int_{p_1}^{p_2} R_d \Delta T d \ln p = - \oint R_d T d \ln p \quad (3.14)$$

where the line integral on the right follows the parcel going from p_1 to p_2 and the environment going from p_2 to p_1 . This work is generally called the convective available potential energy, or CAPE.

The main disadvantage of the skew T-log p chart is that trajectories of ascending parcels (both dry and moist) follow complex curves rather than straight lines.

3.5.2 Entropy-pressure chart

Figure 3.5 shows an alternate way of plotting a thermodynamic sounding which is useful in the case of moist convection. Total entropy and saturated entropy are plotted against pressure, with auxiliary lines showing contours of potential temperature (or dry entropy) as a function of pressure and saturated entropy. Parcel trajectories of entropy in all cases and saturated entropy in the saturated case follow vertical lines, while trajectories of saturated entropy in the unsaturated case follow lines of constant potential temperature.

The main advantages of this type of chart are that moist ascending parcels follow a simple trajectory and that temperature and moisture effects on parcel instability are presented on commensurate scales. One disadvantage is that the buoyancy of a parcel is harder to determine quantitatively than in a skew T-log p chart. However, the potential temperature contour lines help in this regard.

3.6 References

Hess, S. L., 1959: *Introduction to Theoretical Meteorology*. Holt, Rinehart, and Winston, New York, 362 pp.

3.7 Problems

1. Answer the following questions using the sounding presented on the entropy-pressure chart (figure 3.5):
 - (a) Determine the lifting condensation level of parcels lifted from 1000 hPa.
 - (b) Determine the initial level of neutral buoyancy for a parcel lifted from 1000 hPa.
 - (c) Determine the highest level which exhibits positive parcel buoyancy upon lifting.
 - (d) Determine the level of free convection (i. e., the first level at which the buoyancy becomes positive) for parcels originating at 950 hPa.

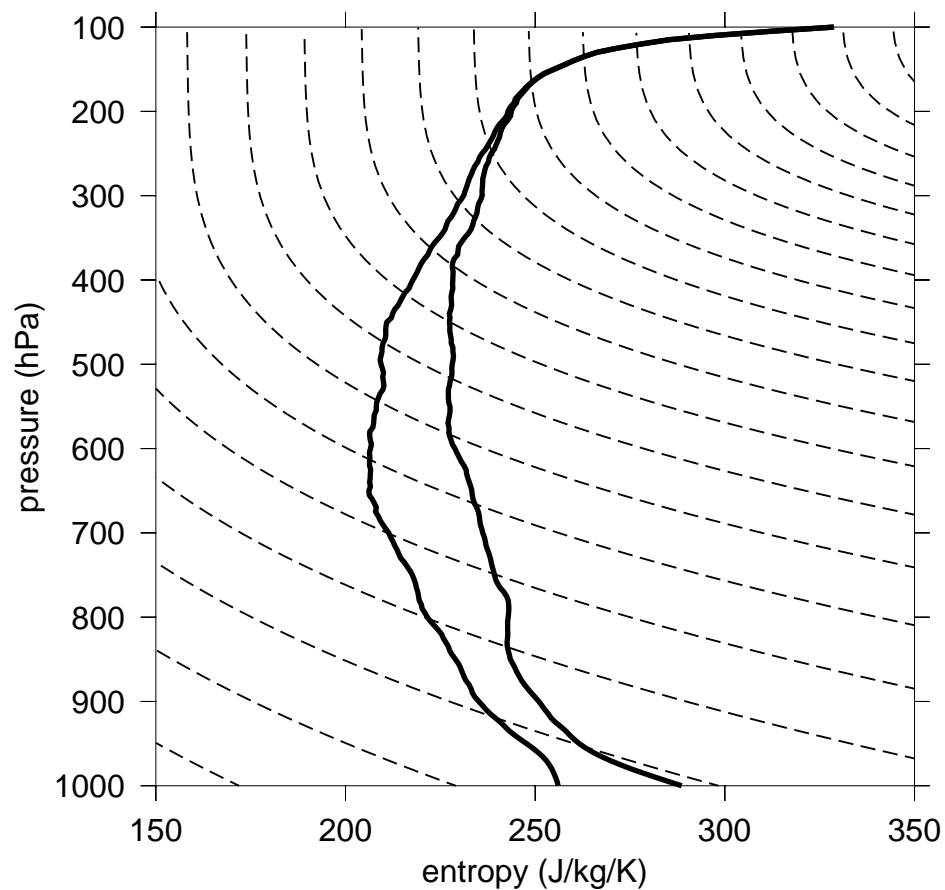


Figure 3.5: Entropy-pressure chart of mean east Pacific sounding, as in figure 3.4. The left curve shows the total entropy while the right curve shows the saturated entropy. The dashed lines show contours at 5 K intervals of potential temperature as a function of the pressure and the saturated entropy.

- (e) A parcel starting at 700 hPa is cooled by 10 K in potential temperature by evaporation of precipitation. What is its new level of neutral buoyancy?